Linear Energy Relationships for the Octahedral Preference of Mg, Ca and Transition Metal Ions

George Pontikis, James Borden, Václav Martínek,† and Jan Florián*

Department of Chemistry, Loyola University Chicago, Chicago, Illinois 60626

Received: October 9, 2008; Revised Manuscript Received: January 27, 2009

The geometry, atomic charges, force constants, and relative energies of the symmetric and distorted $M^{2+}(H_2O)_4(F^-)_2$, $M^{3+}(H_2O)_4(F^-)_2$, $M^{2+}(H_2O)_3(F^-)_2$, and $M^{3+}(H_2O)_3(F^-)_2$ metal complexes, M = Mg, Ca, Co, Cu, Fe, Mn, Ni, Zn, Cr, V, were calculated by using the B3LYP/TZVP density functional method in both gas phase and aqueous solution, modeled using the polarized continuum model. The deformation energy associated with moving one water ligand 12° from the initial "octahedral" arrangement, in which all O−M−O, O−M−F, and F−M−F angles are either 90° or 180°, was calculated to examine the angular ligand flexibility. For all $M^{2+}(H_2O)_4(F^-)_2$ complexes, this distortion increased the energy of the complex in proportion to the electrostatic potential-derived (ESP) charge of the metal, and in proportion to D^{-10}, where D is the distance from the distorted ligand to its closest neighbor. The octahedral stability was further examined by calculating the energies for the removal of a water ligand from the octahedral complex to form a square-pyramidal or trigonal-bipyramidal complex. The octahedral preference, defined as the negative of the corresponding binding energy of the ligand, was found to linearly correlate with the ESP charge of the metal in both the gas phase and aqueous solution. The obtained results indicate that quantum-mechanical covalent effects are of secondary importance for both the flexibility and the octahedral preference of $M^{2+}(H_2O)_4(F^-)_2$ and $M^{3+}(H_2O)_4(F^-)_2$ complexes. This conclusion and supporting data are important for the development of consistent molecular mechanical force fields of the studied metal ions.

1. Introduction

Metal ions participate in biochemical catalysis,[1−3] often forming distorted octahedral complexes in the active site.[4] An important catalytic role of metal ions is to stabilize the negative charges of their ligands, including substrate transition states, or OH^- and RO^- nucleophiles at neutral pH.[5−8]

Most metal carcinogens decrease the fidelity of DNA replication.[9] This fidelity decrease is largely due to increasing the rate of insertion of incorrect deoxyribonucleotide substrates without affecting the insertion of correct deoxyribonucleotide substrates, or exonuclease proofreading activity of DNA polymerases.[10] To gain structural and mechanistic understanding of this interesting substrate dependence of the metal-catalyzed enzyme activity, simulations of DNA polymerase functions[11] need to be carried out with a computational method capable of factoring in the differences in the electronic structure of transition metals.

Since the accurate quantification of metal catalytic effects requires averaging energies of a large number of configurations of an enzyme−substrate−solvent system,[12,13] we must resort to fast computational methods that compromise on the accuracy of their potential energy surfaces. The most promising approach involves the combination of a quantum-mechanical and molecular-mechanical description of the potential energy surface.[14−16] To set a rigorous foundation for the parametrization of molecular mechanical force fields of metalloenzymes,[17] high-level quantum mechanical calculations of the structure and energetics of a consistent series of metal complexes are needed.

Previous quantum mechanical studies explored the geometric and energetic changes in Mg(II),[18−23] Cu(II),[24,25] Co(III),[26] Mn(II) and Mn(III),[23] Fe(II) and Fe(III),[27] and Zn(II)[20,23,28] complexes, generated by variations in the total spin or ligand identity. However, systematic comparisons over the third-period metal series have been scarce.[29]

In this study, we investigate the geometric and energetic properties of the $M^{2+}(H_2O)_4(F^-)_2$ and $M^{3+}(H_2O)_4(F^-)_2$ complexes in the gas phase, and in aqueous solution modeled by the dielectric continuum. Our choice of the small F^- and H_2O ligands reduces the magnitude of steric interligand interactions to ensure that the calculations reflect the intrinsic chemical properties of the metal. In addition, large solvation effects were avoided by working with electroneutral ($M^{2+}(H_2O)_4(F^-)_2$) or +1 charged ($M^{3+}(H_2O)_4(F^-)_2$) complexes. Such a simple yet reasonably realistic model system has produced several simple relationships between the structural and energetic parameters. These relationships can be used as constraints in the design of transferable force fields, aiding established data such as metal−ligand distances[30] or solvation free energies.[31,32]

2. Computational Methods

The gas phase electronic structure calculations and geometry optimization of the studied complexes were carried out at the B3LYP/TZVP level. B3LYP is a density functional method, which consists of Becke's three-parameter hybrid gradient corrected exchange functional[33] combined with the gradient-corrected correlation functional of Lee, Yang, and Parr.[34] These functionals operated on the electron density that was expanded by using the TZVP triple-ζ valence polarized basis set of Ahlrichs and co-workers.[35] Our selection of a basis set that lacks diffuse functions is reasonable because the studied complexes do not carry an overall negative charge. Moreover, our results were obtained by moving or removing neutral water ligand,

* To whom correspondence should be addressed. E-mail: jfloria@luc.edu.
† Permanent address: Department of Biochemistry, Faculty of Science, Charles University, Albertov 2030, 12840 Prague, Czech Republic.

10.1021/jp808928f CCC: $40.75
Published on Web 03/26/2009

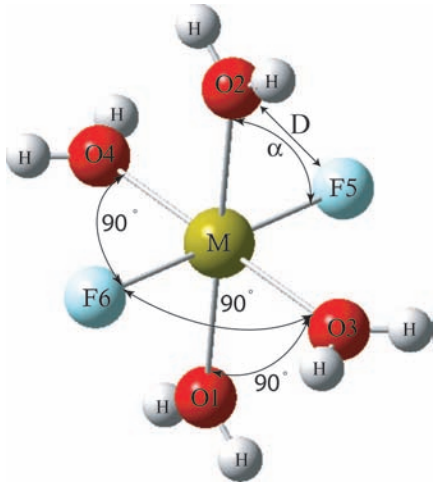

Figure 1. The model system used to study the octahedral preference of various metals with the utilization of four water and two fluoride ligands. Although the ideal octahedron implies the O_h symmetry and premises equivalence of all ligands, throughout this paper we use the term octahedral (OCT) to reflect the angular symmetry of the metal bonds to its ligands.

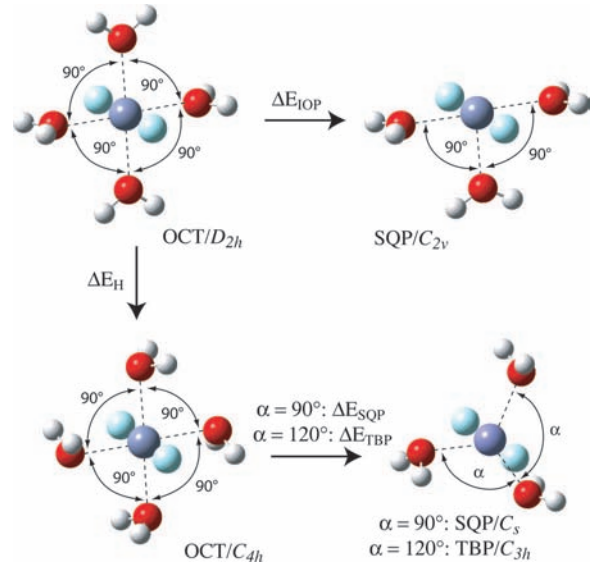

Figure 2. Structures and symmetries of metal complexes used to calculate energetics of the water ligand removal from the octahedral geometry as it proceeds to a square pyramidal (SQP) or trigonal bipyramidal (TBP) geometry. Metal ion (dark blue)−fluoride (light blue) bonds are perpendicular to the plane intersecting oxygen atoms (red).

while keeping the bonding to F^- unchanged. The negligible effects of diffuse basis functions were confirmed for the $[Zn(F)_2(H_2O)_4]$ complex, where extra diffuse basis functions on O (exponent 0.05) and F (exponent 0.062) atoms resulted in a bond increment of only 0.004 Å. Additional calculations were carried out by using the ab initio MP2/TZVP and CCSD(T)/TZVP methods. Gaussian 03[36] was employed in all calculations.

The flexibility of a water position in the octahedral metal complexes was studied via the geometry optimization of structures containing a deformed O−M−F angle, which is denoted as α in Figure 1. The distortion was induced by constraining α at 87° and 78°, while keeping the remaining metal−ligand bond angles and dihedral angles involving hydrogen atoms at their octahedral values of 0°, 90°, or 180° (Figure 1). All remaining geometric parameters were allowed to fully relax. The hydrogen atoms of the mobile water ligand were constrained in an orientation perpendicular to the plane of the three atoms forming the deformed angle. This conformation was chosen to minimize the contribution of ligand−ligand interactions to the calculated deformation energies, and led to an octahedral reference state with a rhombic distortion (OCT/D_{2h}, Figure 1). The geometry optimizations were carried out in internal coordinates defined by the *Z*-matrix formalism, using the Berny algorithm.[37]

The energy required for the removal of a water ligand was calculated for the same initial state (OCT/D_{2h}) and the final state corresponding to the square-pyramidal complex with C_{2v} symmetry (SQP/C_{2v}). That is, from the two nonequivalent pairs of water ligands in the OCT/D_{2h} structure, we removed the ligand with OH bonds pointing to O3 and O4 oxygen atoms (Figure 1). In the resulting SQP/C_{2v} state, all metal−ligand angles and dihedral angles to H atoms retained their values from the OCT/D_{2h} state. The *Z*-matrices used for constrained optimizations of the OCT and SQP states are presented in Tables 1S and 2S in the Supporting Information.

To include the contribution of ligand−ligand interactions to the energy for the removal of a single water ligand, we removed one of the four equivalent water molecules from the initial six-coordinated state of the C_{4h} symmetry (OCT/C_{4h}) to arrive at the five-coordinated states defined as square-pyramidal (SQP/C_s) and trigonal-bipyramidal (TBP/C_{3h}) complexes (Figure 2, also Table 3S in the Supporting Information). For each complex, the OCT/C_{4h} structure was more stable than the OCT/D_{2h} one, the former representing true minimum (confirmed by all positive eigenvalues of the Hessian matrix) for $M^{3+}(H_2O)_4(F^-)_2$ complexes, but only the lowest stationary state of the given symmetry for $M^{2+}(H_2O)_4(F^-)_2$ complexes. For all complexes, the normal vibrations corresponding to negative eigenvalues of the Hessian matrix were confirmed to correspond to the constrained degrees of freedom.

Free energies in aqueous solution were determined by combining the integral equation formalism implementation of the polarized continuum model (IEF-PCM)[38] with the B3LYP/TZVP description of the electronic structure of the solute and B3LYP gas phase solute geometries. This level of theory will be further denoted as IEF-PCM/B3LYP/TZVP//B3LYP/TZVP. The default united atom solute−solvent boundary and IEF-PCM parameters provided by the Gaussian 03 program[36] were employed.

The atomic charges were fitted by using the B3LYP/TZVP electrostatic potential of the solute and the POP=(mk,dipole,readradii) keyword. The default Pauling atomic radii were used in these calculations for all atoms except the metals for which the Pauling radius was scaled by a factor of 1.2. This scaling was done in order to keep the grid points, which determine the atomic charges, outside the solute. This procedure resulted in the following set of radii (Å):[32] Ca (1.188), Co (0.89), Cu(0.91), Cr (1.01), Fe (0.91), Mg (0.78), Mn (0.96), Ni (0.86), V (1.06), Zn (0.89). The same atomic radii were used for all oxidation and spin multiplicity states for each metal with the exception of V(V), for which a radius of 1.7 Å was used to make it consistent with our previous study of vanadate esters.[39] Atomic charges determined by this procedure are well suited for describing intermolecular interactions. The effect of aqueous solvation on atomic charges was evaluated for selected complexes. The solvation was found to increase the absolute value of the charges on the metal and F ligands by 5−8%, but left the overall charge of the water ligands unchanged.

TABLE 1: Energetics of Metal Complexes[a] in Gas Phase and Aqueous Solution

	gas phase (kcal/mol)[b]				aqueous solution (kcal/mol)[c]			
metal	ΔE_{IOP}	ΔE_H	ΔE_{SQP}	ΔE_{TBP}	ΔG_{IOP}	ΔG_H	ΔG_{SQP}	ΔG_{TBP}
Ca(II)	10.1	−8.7	14.5	12.2	5.4	−1.1	5.5	11.9
Co(II) (h.s.)	6.1	−15.7	14.5	24.4	5.8	−3.9	7.0	14.7
Co(III) (h.s.)	24.0	−5.9	27.6	37.9	12.4	−3.3	13.7	27.8
Cr(III) (h.s.)	31.0	−11.4	36.9	40.0	18.4	−5.8	20.9	36.4
Cu(II)[b]	0.7	−17.5	9.6	9.5	2.9	−5.1	4.8	4.1
Fe(II) (h.s.)	4.2	−13.4	11.4	24.2	4.3	−3.1	5.1	15.4
Fe(III) (h.s.)	23.4	−8.8	28.2	21.7	10.6	−4.9	13.8	17.4
Mg(II)	7.3	−15.3	16.3	12.8	6.6	−3.6	8.3	8.2
Mn(II) (h.s.)	3.6	−12.6	10.6	9.5	2.7	−3.4	4.4	6.5
Ni(II)	5.6	−20.2	16.0	19.5	5.6	−7.1	8.2	10.0
V(III) (h.s.)	31.1	−5.2	41.9	36.1	18.1	0.0	37.9	32.9
V(V) O2[d]	23.7	−20.2	33.2	23.0	13.2	−14.7	19.4	18.2
Zn(II)	2.9	−16.0	12.0	10.4	2.3	−5.5	4.5	5.5

[a] Figure 2. [b] Gas phase results are presented in terms of energy differences because some structures did not support consistent evaluation of entropic contributions using harmonic approximation due to our use of octahedral constraints for complexes containing different ligands (see also Computational Methods): $\Delta E_{IOP} = E(SQP/C_{2v}) + E(H_2O) - E(OCT/D_{2h})$, $\Delta E_H = E(OCT/C_{4h}) - E(OCT/D_{2h})$, $\Delta E_{SQP} = E(SQP/C_s) + E(H_2O) - E(OCT/C_{4h})$, $\Delta E_{TBP} = E(TBP/C_{3h}) + E(H_2O) - E(OCT/C_{4h})$, $E(H_2O) = -76.460622$ au. [c] The solvation energetics was calculated in terms of PCM solvation free energies (ΔG_{solv}, Table 6S in the Supporting Information). The sum of gas phase energies and solvation free energies is then labeled, in accordance with common practice in the literature (see, e.g., ref 56 and references therein), as ΔG: $\Delta G = \Delta E + \Delta\Delta G_{solv}$, $\Delta G_{solv}(H_2O) = -6.2$ kcal/mol. [d] $F5^-$ and $F6^-$ are replaced by O^{2-}.

3. Results and Discussion

3.1. Octahedral Preference. The intrinsic preferences of 2+ and 3+ metals for a coordination number six were assessed by evaluating the energy needed to remove a water ligand from an octahedral metal complex while allowing only the M−L and O−H bond distances and intramolecular HOH angles to relax upon the ligand removal (Table 1). The analysis of energies (cf. Tables 4S and 5S in the Supporting Information) and geometries of octahedral compounds of D_{2h} and C_{4h} symmetry has shown that water ligands with hydrogen atoms pointing toward fluoride ions are more stabilized by ligand−ligand interactions than water ligands with their hydrogen atoms pointing to oxygen atoms. For example, the Zn−O2 bond (Figure 1) contracted from 2.38 to 2.27 Å upon going from D_{2h} to C_{4h} symmetry (Figure 2). The increase in the number of H-atoms upon replacing the two fluoride ligands by water molecules resulted in a further shortening of the Zn−O bond to 2.13 Å. These geometric changes underscore the important role of hydrogen-mediated ligand−ligand interactions in the stability of the metal complexes.

Since these interactions tend to obscure intrinsic metal properties we selected the octahedral D_{2h} complex (Figure 1, OCT/D_{2h}) as our reference state for the investigation of intrinsic metal octahedral preference and octahedral flexibility. The comparison of absolute energies of these complexes (Table 4S, Supporting Information) singles out their high-spin state as more stable than the low-spin state for all 3d transition metals. This result is consistent with the fact that the H_2O and F^- ligands are considered to be "weak" ligands in the framework of crystal field theory.[40] Nevertheless, the high-spin preference of Co(II) and Co(III) complexes is tenuous. For example, the high-spin state of the six-coordinated complex of Co(II) with D_{2h} symmetry can be transformed to low-spin by a mere reorientation of its two H_2O ligands to form D_{4h} complex (which has higher total energy than D_{2h}). Similarly, while the high-spin state is more stable for $[Co(H_2O)_4F_2]^+$ (D_{2h}), which has its F^- ligands in the trans orientation, the low-spin state is more stable for the cis isomer of this complex.

TABLE 2: Atomic Charges[a] of the SQP/C_{2v} and OCT/D_{2h} Complexes

	square pyramidal				octahedral		
metal	metal	F	H_2O[b]	H_2O[c]	metal	F	H_2O
Ca(II)	1.776	−0.88	−0.02	0.02	1.95	−0.89	−0.08
Co(II) (h.s.)	1.417	−0.68	−0.06	0.07	1.84	−0.75	−0.11
Co(III) (h.s.)	1.665	−0.43	0.03	0.13	1.91	−0.47	−0.02
Cr(III) (h.s.)	1.918	−0.58	0.05	0.13	1.93	−0.59	0.04
Cu(II)	1.125	−0.63	0.04	0.04	1.66	−0.71	−0.12
Fe(II) (h.s.)	1.274	−0.65	−0.02	0.06	1.84	−0.73	−0.13
Fe(III) (h.s.)	1.763	−0.5	0.05	0.12	1.97	−0.54	−0.02
Mg(II)	1.704	−0.81	−0.06	0.03	2.03	−0.86	−0.12
Mn(II) (h.s.)	1.282	−0.67	0	0.06	1.69	−0.74	−0.09
Ni(II)	1.428	−0.72	−0.04	0.07	1.77	−0.76	−0.11
V(III) (h.s.)	1.952	−0.56	0.01	0.12	1.94	−0.55	0.03
V(V) O_2[d]	2.031	−0.61	0.21	0.19	2.12	−0.71[d]	0.01
Zn(II)	1.280	−0.65	−0.02	0.06	1.75	−0.73	−0.11

[a] ESP charges (B3LYP/TZVP). [b] Equatorial ligand. [c] Axial ligand. [d] $F5^-$ and $F6^-$ are replaced by O^{2-}.

B3LYP is prone to favor high-spin states for octahedral complexes of Fe(II) with PMe_3 ligands in combination with N and S, but predicts the correct low-spin states for similar complexes where PMe_3 is replaced by CO or NO^+.[41] Although there are ongoing efforts to improve the DFT methodology for transitional metals leading to new functionals such as O3LYP[42] or MO6,[43] it was noted by Baker and Pulay that there is no real incentive to use either OLYP or O3LYP in place of B3LYP for calculations involving first-row transition metals.[42] In addition, due to its widespread use, the B3LYP functional represents the method of first choice for comparative studies. Here we compared B3LYP with more accurate ab initio MP2 calculations for Fe(II) and Co(II) complexes, but MP2 showed even greater preference for the higher spin state than the B3LYP method (Table 4S, Supporting Information). In further evaluating the credibility of the B3LYP method, we compared B3LYP/TZVP and CCSD(T)/TZVP//B3LYP/TZVP energies for ligand removal from Mg(II), Ca(II), Mn(II), Zn(II), Ni(II), Cu(II), Fe(III), and Co(III) octahedral complexes (Table 5S, Supporting Information). While the coupled-cluster method favored the octahedral state by an extra 1 to 2 kcal/mol for 2+ metals and 3 to 4 kcal/mol for 3+ metals, the relative energies within groups of 2+ and 3+ metals were affected by less than 1 kcal/mol.

When quantum-mechanical charges of 2+ metal ions are considered (Table 2), the intrinsic metal octahedral preference, defined as $\Delta E_{IOP} = E(SQP/C_{2v}) + E(H_2O) - E(OCT/D_{2h})$ where E denotes the gas-phase energy, increases linearly with the magnitude of the metal charge (Figure 3, top). This relationship, which is characterized by a correlation coefficient of 0.96, uses metal charges from SQP/C_{2v} complexes because the location of the metal on the solvent-accessible surface in these complexes results in the smallest charge uncertainty.[44] Although the metal charges significantly increase upon going from SQP to OCT complexes (Table 2) the linear dependence of ΔE_{IOP} is retained for metal charges calculated by averaging ESP charges of OCT/D_{2h} and SQP/C_{2v} complexes ($R = 0.94$, not shown in Figure 3). The propensity of ΔE_{IOP} to increase with the metal charge is substantiated by data for 3+ metals, which show significantly larger metal charges and ΔE_{IOP} than 2+ metals (Table 1). Moreover, within the group of 3+ metals, ΔE_{IOP} also grows with increasing metal charge.

The validity of a simple relationship of Figure 3A is promising for the development of consistent molecular mechan-

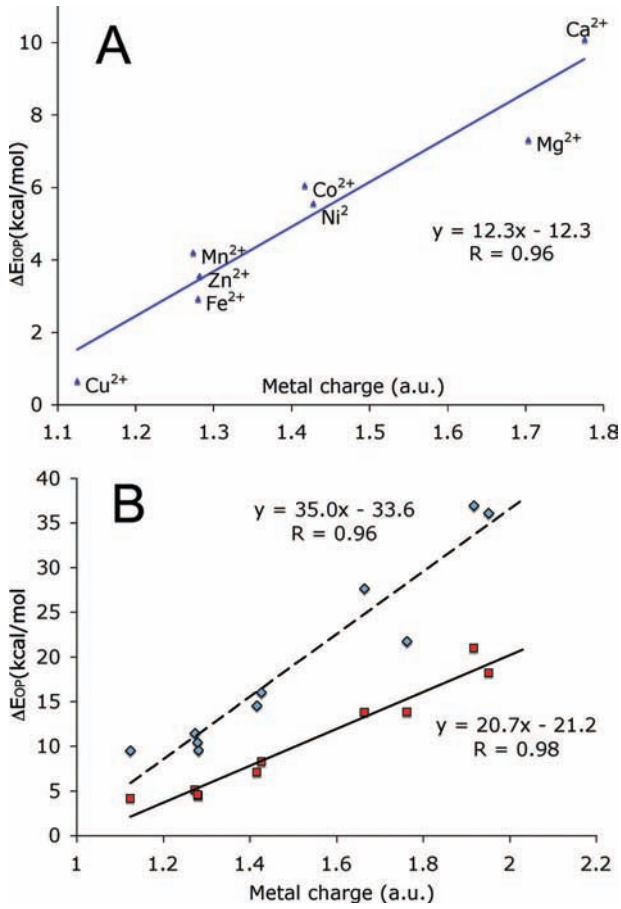

Figure 3. Top (A): Correlation between the intrinsic metal octahedral preference, ΔE_{IOP} (Figure 2, Table 1), and the ESP-derived charge of the metal in the SQP/C_{2v} complex. Bottom (B): Correlation between the metal octahedral preference (eq 1) and the ESP-derived charge of the metal in the SQP/C_{2v} complex in the gas phase (blue dimonds, dashed line) and aqueous solution ($\Delta G_{OP} = \Delta E_{OP} + \Delta\Delta G_{solv}$, red squares, full line).

ics force fields for 2+ metals because it indicates the dominant role of classical electrostatic rather than quantum-mechanical covalent effects in the stability of transition metal complexes. It is, however, possible that metal−ligand covalent bonding participates to a greater extent in stabilizing OCT/C_{4h} complexes, which show extra stabilization via hydrogen-mediated interligand interactions. The likelihood of coupling of metal−ligand covalent interactions with ligand−ligand interactions is corroborated by the fact that the magnitude of hydrogen-mediated ligand stabilization (E_H, Table 1 and Figure 2) of 2+ metal complexes does not correlate with the metal−O2 bond length of OCT/D_{2h} complexes ($R = 0.65$).

If the H_2O ligand that forms hydrogen bonds with the F^- ligands (Figure 2, OCT/C_{4h}) is removed and the remaining ligands are allowed to relax to the SQP/C_s, SQP/C_{2v}, or TBP/C_{3h} state, the resulting octahedral preference

$$\Delta E_{OP} = min[E(SQP/C_s), E(SQP/C_{2v}), E(TBP/C_{3h})] + E(H_2O) - E(OCT/C_{4h}) \quad (1)$$

still correlates with the metal charge (Figure 3, bottom). The trigonal-bipyramidal geometry is favored by all studied metals, with the exception of Co^{2+}, Co^{3+}, Cr^{3+}, Fe^{2+}, and Ni^{2+}. Although the energy of some six- or five-coordinated complexes could be further lowered by relaxing their symmetry, the heterogeneity in angles and torsional angles of C_1 complexes would prevent consistent comparison of metal−ligand interactions because these interactions would be obscured by the differences in the energetics of interligand interactions.

In solution, removing a water ligand from the OCT complexes exposes the metal to the solvent, and makes the solute smaller in both the SQP and TBP arrangements. Since the solvation free energy (ΔG_{solv}) is inversely proportional to the radius of the sphere that encloses the complex,[45] smaller SQP and TBP complexes are better stabilized by solvation than larger OCT complexes (Table 6S, Supporting Information). The same solvation trend could be inferred by considering a nonspherical solute in a dipolar solvent model[46] because the solvent dipoles come closer to the atom with the highest charge density (i.e., metal) in a five-coordinated than in a six-coordinated complex. Thus, the octahedral preference decreases upon moving the complexes into aqueous solution. Since ΔG_{solv} is also proportional to the square of the charge of the solute,[45] the octahedral preference of 3+ complexes is affected to a greater extent than that of 2+ complexes. In addition, since metals in the SQP state are more exposed to solvent, 5-coordinate 3+ complexes prefer SQP over TBP geometry, while the calculated free energy differences between 5-coordinate (SQP or TBP) 2+ complexes are generally small (Table 1). The latter result is consistent with the observation that many molecules with five ligands either have structures between TBP and SQP or can switch easily from one structure to the other.[47] The correlation between octahedral preference and metal charge is reinforced in aqueous solution (Figure 3, bottom), because the ligand−ligand interactions are weakened by solvation effects.

Calcium and magnesium metals having no d-electrons were excluded from the correlated data (Figure 3, bottom). Nevertheless, it is interesting to note that both Ca^{2+} and Mg^{2+} tend to have significantly smaller ΔE_{OP} than transition metals of the same charge. In Ca^{2+}, this behavior is consistent with its large ionic radius, fast observed ligand-exchange rates, and flexible coordination sphere that can accommodate seven or eight ligands.[48,49]

Cu^{2+} has the least stable OCT arrangement in both the gas phase and solution. This result is consistent with the large propensity of octahedral Cu^{2+} complexes to lower their energy by lowering their symmetry due to the Jahn−Teller effect,[50] in the extreme case preferring the square-planar structure. This finding agrees with experimental findings from CSD and PDB analyses, showing Cu^{2+} preferring coordination numbers of five and four.[51,52] Interestingly, the low OCT preference of Cu^{2+} is also consistent with its low ESP charge (Figure 3), which is closer to +1 rather than +2, despite the Cu oxidation state being +2. This large transfer of electron density toward the metal center, which allows Cu^{2+} to achieve electron distribution that is close to completely filled d-orbitals, has been previously calculated for Cu^{2+} complexes with biological ligands such as DNA bases or amino acids.[53,54]

3.2. Distortion of the Octahedral Complexes. The octahedral deformation energies, $\Delta E\ (78°) = E(78°) - E(90°)$, evaluate the destabilization in going from a D_{2h} geometry to a distorted one (Figure 1, Table 3, and Table 4S (Supporting Information)). The calculated deformation energies of the complexes with 2+ metals are less than 2.2 kcal/mol. This energy increase is only marginally larger than the mean thermal energy (RT) of 0.6 kcal/mol at $T = 298$ K. This comparison, in addition to small deformation harmonic force constants (Table 3), shows that the studied metal complexes are very flexible.

TABLE 3: Structure and Energetic Parameters for Distorting the M^{n+} Complexes (Figure 1)

				M−L distance[d] (Å)		
metal	$\Delta E(78°)$[a] (kcal/mol)	k[b] (kcal/mol/Rad^2)	$\Delta E_{HO}(78°)$[c] (kcal/mol)	M−F5 (90°)	M−O2 (90°)	M−O2 (78°)
Ca(II)	0.9	60.6	1.3	2.20	2.53	2.55
Co(II) (h.s.)	2.1	130.9	2.9	1.89	2.23	2.30
Co(III) (h.s.)	3.2	158.3	3.5	1.77	2.13	2.18
Cr(III) (h.s.)	3.6	191.4	4.2	1.83	2.07	2.11
Cu(II)	1.2	68.2	1.5	1.84	2.45	2.65
Fe(II) (h.s.)	1.7	98.3	2.2	1.87	2.33	2.41
Fe(III) (h.s.)	2.9	139.7	3.1	1.81	2.18	2.23
Mg(II)	2.2	116.3	2.5	1.88	2.24	2.32
Mn(II) (h.s.)	1.4	71.2	1.6	1.92	2.44	2.52
Ni(II)	2.2	156.8	3.4	1.90	2.21	2.27
V(III) (h.s.)	3.5	174.9	3.8	1.83	2.10	2.14
V(V) O_2[e]	4.6	215	4.7	1.68[e]	2.16	2.24
Zn(II)	1.6	88.8	1.9	1.85	2.38	2.49

[a] The relative energy of the system, $\Delta E(78°) = E(78°) - E(90°)$, where $E(\theta)$ denotes the total energy of the complex calculated for the α angle constrained at a value θ. $E(90°)$ energies refer to structures with D_{2h} symmetry. [b] The force constant as defined by the equation $k = 2(E(87°) - E(90°))/x^2$, where x is defined as the displacement angle from $\alpha = 90°$ in radians. [c] ΔE_{HO} is the relative energy at $\alpha = 78°$ calculated by using the harmonic oscillator approximation with the reported force constant. [d] The bond distance between the metal and the specified ligand. [e] $F5^-$ and $F6^-$ are replaced by O^{2-}.

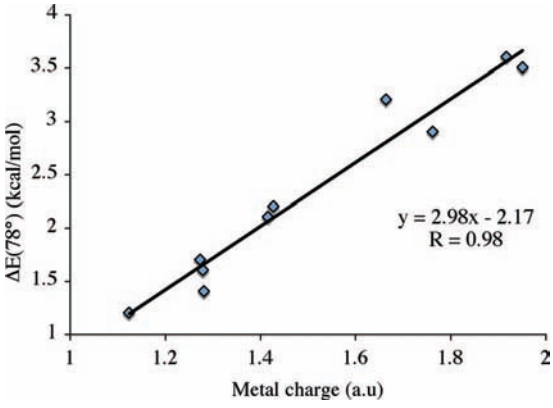

Figure 4. Correlation between the octahedral deformation energies (Table 3) and the ESP-derived metal charges in the SQP/C_{2v} complex.

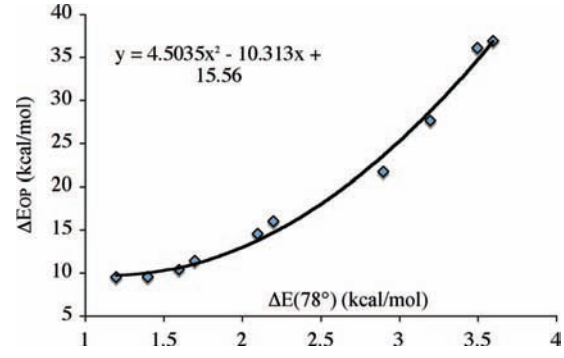

Figure 5. Correlation between the metal octahedral preference (eq 1) and the octahedral deformation energy.

The effect of a ligand loss or distortion on the atomic charges can be scrutinized by comparing data in Tables 2 and 7S (Supporting Information). In all cases, metal charges decrease in proceeding from OCT to SQP. The subsequent relaxation of the ligands from SQP to TBP causes a partial return of the charges on the 2+ metals to their original OCT values but charges of 3+ metals are further decreased. The 12° angular distortion induces a decrease in the charge of the metals by 0.1 to 0.3 au due to the transfer of electron density from the ligands to the metal.

Metals with a 3+ charge were found to have a greater intrinsic rigidity than 2+ metals, indicating that a linear correlation similar to the one for octahedral preference might hold. Indeed, when octahedral deformation energies were plotted as a function of the quantum-mechanical charge of the metal (Figure 4) we obtained a linear relationship characterized by a correlation factor of 0.98. This correlation is again based on the ESP-derived metal charges of the SQP complexes. Since we showed that the same metal charges correlate with both octahedral preference and deformation energies, the latter two quantities are also mutually correlated (Figure 5). However, instead of a weak linear correlation ($R = 0.95$, not shown in Figure 5) the data are more fittingly characterized by a quadratic function. The high correlation coefficient of 0.996 for this relationship indicates that the deformation energies of octahedral complexes of third-row transition metals represent nearly perfect measure of their stability with respect to a loss of their ligand. Given the prevalent role of linear free-energy relationships in the kinetics of associative and dissociative mechanisms for ligand exchange (see, e.g. ref 55 and references therein) it is likely that $\Delta E(78°)$ values of transition metals could also correlate with the rate constants for ligand exchange.

Unlike for the energetics of the complete ligand loss where the correlations of Figure 3 stem from the direct electrostatic interactions, octahedral deformation energies are likely to be connected to the metal charge indirectly via changes in metal−ligand and ligand−ligand distances. The bond from the metal to the displaced water ligand lengthens in proceeding from $\alpha = 90°$ to 78° (Table 3, Figure 1). The bond to F5 also becomes slightly extended due to this distortion while the bonds to the remaining ligands become shorter (Table 8S, Supporting Information). As the distance between the ligands (D, Figure 1) decreases upon going from 2+ to 3+ complexes, $\Delta E(78°)$ increases. The best linear correlation ($R = 0.996$) was achieved when plotting $\Delta E(78°)$ as a function of $1/D^{10}$ (Figure 6), but a very good correlation coefficient of 0.98 was also achieved for $1/D^2$. These correlations and the lack of metal-specific outliers (both Mg^{2+} and Ca^{2+} are included in Figure 6) indicate that the distortion energy of each complex is determined by a combination of electrostatic and steric interligand repulsions over any intrinsic covalent effects. However, given the nature of the studied complexes this conclusion is limited to ligands forming ionic metal−ligand bonds. The distortion behavior described here is likely to be accurately modeled by using classical molecular mechanic potentials.

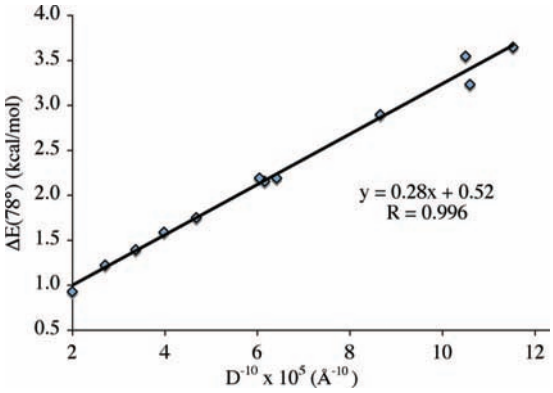

Figure 6. Correlation between the deformation energy of the octahedral complexes and D^{-10}, where D is the interligand distance (Figure 1).

4. Conclusions

Our systematic computational analyses regarding the stability and electronic structure of octahedral $M^{n+}(H_2O)_4(F^-)_2$ complexes indicate that their distortion energetics are dominated by electrostatic and steric interactions rather than intrinsic covalent effects (associated with the electronic structure of the metal). Because the metal electronic structure affects the distortion energetics indirectly, via the bond distances, it should be feasible to generate consistent molecular mechanical force fields for Mg^{2+}, Ca^{2+}, and most of the third-period transition metals. This approach could treat the angular deformations of the complexes with reasonable accuracy. The octahedral preference of the metals (measured by the energy associated with a loss of one water ligand) depends strongly on the metal oxidation state and electronic structure. Metals in the 3+ oxidation state show a higher preference for the octahedral state than 2+ metals. This observation was generalized by showing that the octahedral preference of metal ion complexes in the gas phase was proportional to the atomic charge of the metal. The presented bond lengths, force constants, atomic charges, and energetic data of the $M^{n+}(H_2O)_4(F^-)_2$ complexes will provide benchmarks for the development of the classical and polarizable force fields of metal ions.

Acknowledgment. This work was supported by the Research Innovation Award from Research Corporation and by the NIH grant 1U19CA105010.

Supporting Information Available: Spin multiplicities, total energies, bond lengths, and atomic charges for the octahedral and deformed octahedral complexes and Gaussian input files for the calculations of geometries, normal vibrational modes, ESP atomic charges, and PCM solvation free energies. This material is available free of charge via the Internet at http://pubs.acs.org.

References and Notes

(1) Williams, R. J. P. *Pure Appl. Chem.* **1982**, *54*, 1889.
(2) Sträter, N.; Lipscomb, W. N.; Klabunde, T.; Krebs, B. *Angew. Chem., Int. Ed. Engl.* **1996**, *35*, 2024.
(3) Trawick, B. N.; Daniher, A. T.; Bashkin, J. K. *Chem. Rev.* **1998**, *98*, 939.
(4) Batra, V. K.; Beard, W. A.; Shock, D. D.; Krahn, J. M.; Pedersen, L. C.; Wilson, S. H. *Structure* **2006**, *14*, 757.
(5) Fersht, A. R. *Structure and Mechanism in Protein Science*; W. H. Freeman and Company: New York, 1999.
(6) Jenkins, L. A.; Bashkin, J. K.; Pennock, J. D.; Florián, J.; Warshel, A. *Inorg. Chem.* **1999**, *38*, 3215.
(7) Florián, J.; Goodman, M. F.; Warshel, A. *J. Am. Chem. Soc.* **2003**, *125*, 8163.
(8) Yatsimirsky, A. K. *Coord. Chem. Rev.* **2005**, *249*, 1997.
(9) Sirover, M. A.; Loeb, L. A. *Science* **1976**, *194*, 1434.
(10) Zakour, R. A.; Kunkel, T. A.; Loeb, L. A. *Environ. Health Perspect.* **1981**, *40*, 197.
(11) Florián, J.; Goodman, M. F.; Warshel, A. *Proc. Natl. Acad. Sci. U.S.A.* **2005**, *102*, 6819.
(12) Olsson, M. H. M.; Hong, G. Y.; Warshel, A. *J. Am. Chem. Soc.* **2003**, *125*, 5025.
(13) Deeth, R. J. *Inorg. Chem.* **2007**, *46*, 4492.
(14) Warshel, A.; Levitt, M. *J. Mol. Biol.* **1976**, *103*, 227.
(15) Bentzien, J.; Muller, R. P.; Florián, J.; Warshel, A. *J. Phys. Chem. B* **1998**, *102*, 2293.
(16) Rosta, E.; Klahn, M.; Warshel, A. *J. Phys. Chem. B* **2006**, *110*, 2934.
(17) Landis, C. R.; Root, D. M.; Cleveland, T. *Rev. Comput. Chem.* **1995**, *6*, 73.
(18) Dudev, T.; Lim, C. *J. Phys. Chem. A* **1999**, *103*, 8093.
(19) Dudev, T.; Cowan, J. A.; Lim, C. *J. Am. Chem. Soc.* **1999**, *121*, 7665.
(20) Kluge, S.; Westong, J. *J. Biochem.* **2005**, *44*, 4877.
(21) Rezabal, E.; Mercero, J. M.; Lopez, X.; Ugalde, J. M. *J. Inorg. Biochem.* **2007**, *100*, 374.
(22) Oelschlaeger, P.; Klahn, M.; Beard, W. A.; Wilson, S. H.; Warshel, A. *J. Mol. Biol.* **2007**, *366*, 687.
(23) Dal Peraro, M.; Spiegel, K.; Lamoureux, G.; Vivo, M. D.; Degrado, W. F.; Klein, M. L. *J. Struct. Biol.* **2007**, *3*, 444.
(24) Deeth, R. J.; Hearnshaw, L. J. A. *Dalton Trans.* **2005**, 3638.
(25) Pavelka, M.; Simanek, M.; Sponer, J.; Burda, J. V. *J. Phys. Chem. A* **2006**, *110*, 4795.
(26) Deeth, R. J.; Foulis, D. L.; Williams-Hubbard, B. J. *Dalton Trans.* **2003**, 3949.
(27) Deeth, R. J.; Fey, N. *J. Comput. Chem.* **2004**, *25*, 1840.
(28) Sakharov, D. V.; Lim, C. *J. Am. Chem. Soc.* **2005**, *127*, 4921.
(29) Rulisek, L.; Havlas, Z. *J. Am. Chem. Soc.* **2000**, *122*, 10428.
(30) Dudev, T.; Lin, Y.; Dudev, M.; Lim, C. *J. Am. Chem. Soc.* **2003**, *125*, 3168.
(31) Marcus, Y. *Ion Properties*; Marcel Dekker, Inc.: New York, 1997.
(32) Florián, J.; Warshel, A. *J. Phys. Chem. B* **1999**, *103*, 10282.
(33) Becke, A. D. *J. Chem. Phys.* **1993**, *98*, 5648.
(34) Lee, C.; Yang, W.; Parr, R. G. *Phys. Rev. B* **1988**, *37*, 2571.
(35) Schaefer, A.; Horn, H.; Ahlrichs, R. *J. Chem. Phys.* **1992**, *97*, 2571.
(36) *Gaussian03M*, revision C.02; Gaussian Inc.: Pittsburgh, PA, 2004.
(37) Schlegel, H. B. *Adv. Chem. Phys.* **1987**, *67*, 249.
(38) Mennucci, B.; Cances, E.; Tomasi, J. *J. Phys. Chem.* **1997**, *101*, 10506.
(39) Borden, J.; Crans, D.; Florián, J. *J. Phys. Chem. B* **2006**, *110*, 14988.
(40) Rayner-Canham, G. *Descriptive Inorganic Chemistry*; W. H. Freeman and Company: New York, 1996.
(41) Reiher, M.; Salomon, O.; Hess, B. A. *Theor. Chem. Acc.* **2001**, *107*, 48.
(42) Baker, J.; Pulay, P. *J. Comput. Chem.* **2003**, *24*, 1184.
(43) Zhao, Y.; Truhlar, D. G. *Acc. Chem. Res.* **2008**, *41*, 157.
(44) Singh, U. C.; Kollman, P. A. *J. Comput. Chem.* **1984**, *5*, 129.
(45) Born, M. *Z. Phys.* **1920**, *1*, 45.
(46) Florián, J.; Warshel, A. *J. Phys. Chem. B* **1997**, *101*, 5583.
(47) Auf der Heyde, T. P. E.; Burgi, H. B. *Inorg. Chem.* **1989**, *28*, 3960.
(48) Shriver, D. F.; Atkins, P. W.; Overton, T. L.; Rourke, J. P.; Weller, M. T.; Armstrong, F. A. *Inorganic Chemistry*, 4th ed.; W. H. Freeman: New York, 2006.
(49) Dudev, T.; Lim, C. *Chem. Rev.* **2003**, *103*, 773.
(50) Eigen, M. *Ber. Bunsenges. Phys. Chem.* **1963**, *67*, 753.
(51) Dudev, M.; Wang, J.; Dudev, T.; Lim, C. *J. Phys. Chem.* **2006**, *110*, 1889.
(52) Rulisek, L.; Vondrásek, J. *J. Inorg. Biochem.* **1998**, *71*, 115.
(53) Noguera, M.; Bertran, J.; Sodupe, M. *J. Phys. Chem. A* **2004**, *108*, 333.
(54) Bertran, J.; Rodriguez-Santiago, L.; Sodupe, M. *J. Phys. Chem. B* **1999**, *103*, 2310.
(55) Åqvist, J.; Kolmodin, K.; Florián, J.; Warshel, A. *Chem. Biol.* **1999**, *6*, R71.
(56) Strajbl, M.; Florián, J.; Warshel, A. *J. Phys. Chem. B* **2001**, *105*, 4471.

JP808928F